



LAWRENCE  
LIVERMORE  
NATIONAL  
LABORATORY

# **The National Ignition Facility Wavefront Requirements and Optical Architecture**

*M. L. Spaeth, K. R. Manes, C. C. Widmayer,  
W. H. Williams, P. K. Whitman,  
M. A. Henesian, I. F. Stowers, J. Honig*

**June 7, 2004**

Submitted to Optical Engineering

This document was prepared as an account of work sponsored by an agency of the United States Government. Neither the United States Government nor the University of California nor any of their employees, makes any warranty, express or implied, or assumes any legal liability or responsibility for the accuracy, completeness, or usefulness of any information, apparatus, product, or process disclosed, or represents that its use would not infringe privately owned rights. Reference herein to any specific commercial product, process, or service by trade name, trademark, manufacturer, or otherwise, does not necessarily constitute or imply its endorsement, recommendation, or favoring by the United States Government or the University of California. The views and opinions of authors expressed herein do not necessarily state or reflect those of the United States Government or the University of California, and shall not be used for advertising or product endorsement purposes.

# **The National Ignition Facility Wavefront Requirements and Optical Architecture**

M. L. Spaeth, K. R. Manes, C. C. Widmayer, W. H. Williams, P. K. Whitman,

M. A. Henesian, I. F. Stowers, J. Honig

Lawrence Livermore National Laboratory

P.O. Box 808 L-466

Livermore, California 94550

USA

## **ABSTRACT**

With the first four of its eventual 192 beams now executing shots and generating more than 100 kiloJoules of laser energy at its primary wavelength of 1.06  $\mu\text{m}$ , the National Ignition Facility (NIF) at the Lawrence Livermore National Laboratory is already the world's largest and most energetic laser. The optical system performance requirements that are in place for NIF are derived from the goals of the missions it is designed to serve. These missions include inertial confinement fusion (ICF) research and the study of matter at extreme energy densities and pressures. These mission requirements have led to a design strategy for achieving high quality focusable energy and power from the laser and to specifications on optics that are important for an ICF laser. The design of NIF utilizes a multipass architecture with a single large amplifier type that provides high gain, high extraction efficiency and high packing density. We have taken a systems engineering approach to the practical implementation of this design that specifies the wavefront parameters of individual optics in order to achieve the desired cumulative performance of the laser beamline. This presentation provides a detailed look at the causes and effects of performance degradation in large laser systems and how NIF has been designed to overcome these effects. We will also present results of spot size performance measurements that have validated many of the early design decisions that have been incorporated in the NIF laser architecture.

Keywords: Solid-state lasers, fusion lasers

## 1. BACKGROUND

The optical quality or wavefront specifications for the laser slabs, crystals, windows, lenses and mirrors that make up the NIF beamlines were established by flowdown analysis of those that were needed for these components in order to meet the Primary Criteria and Functional Requirements for the NIF laser system. In this paper we will summarize the NIF primary system criteria that are influenced by the wavefront quality of a beamline and then describe how the beamline architecture and specifications for individual optical components have made it possible for NIF to meet its system criteria.

The national motive for building the NIF laser centers around providing a laser driver for three missions of national purpose:

- Inertial Confinement Fusion (ICF)
- The high-energy-density study of materials of interest to the stockpile stewardship program
- The study of materials under very high temperatures and pressures of interest to the scientific community, particularly the astrophysical community

Of these user groups, the one that was most active in establishing the original specifications for NIF was the ICF community; their emphasis for the initial embodiment of NIF was for indirect drive ICF. For this mission, laser light enters a hohlraum through two Laser Entrance Holes (LEH) to irradiate the walls of the hohlraum, subsequently generating x-rays that drive the implosion of a capsule centrally located within the hohlraum.<sup>1</sup>

Thus, the primary wavefront requirement for NIF became its ability to provide focusable energy and power into the laser entrance hole of a hohlraum. The original requirements did not address the character of the distribution of this light within the hohlraum aperture other than to specify the fraction of the light that could be delivered within specified angles consistent with the features of the LEH.

The optical system of the NIF beamlines shown in Figure 1 was chosen because it can meet this need for focusable energy and power. As NIF now comes to life, it is evident that its wavefront quality is meeting and exceeding its

original goals. When NIF is completed it will produce nearly 2 Megajoules of 350 nm light in 192 beams. NIF will be the only terrestrial platform that can concentrate energy and power to levels that approach those in the interiors of stars and nuclear weapons.

It has been recognized for many years that it is the imperfections in the optics of an ICF laser beamline that limit its ability to deliver focused energy to its target. As one would expect from classical and physical optics, phase errors in the optics lead directly to an increase in the size of the focused spot. Ray directions in the laser beam are identical to local gradients of the phase of the propagating wavefront. The gradient of the phase error tolerable for each optic encountered is thus determined by the focal spot size requirement. In addition, because the intensity of the light in the beamline is quite high, amplitude variations in the near-field intensity patterns of the propagating beam can be driven to grow by non-linear effects in the optic, pulling light from the focusable part of the beam and injecting it into a noisy, off-axis fraction of the beam. Without careful attention to keep them under control, these non-linear effects can readily degrade further the ability of the laser to be tightly focused onto the target.

The sequence of images shown in Figure 2 were generated by the LLNL propagation code, PROP,<sup>2</sup> to illustrate the manner in which amplitude variations can be driven by non-linear effects to grow from acceptable to destructive over a relatively narrow range of beamline intensity. Measurements of these phenomena in real high power beams are very similar to those seen in these calculations. Optical phase errors with spatial frequencies higher than about one inverse centimeter as well as small obscurations due to dirt or damage seed the nonlinear parametric loss mechanisms that steal power from the focusable beam. High spatial frequency optical requirements are consequently established to keep these loss mechanisms in check.

The ordinate of the curves in Figure 2 are titled "Contrast." The term Contrast or Spatial Contrast Ratio, is used to quantify nonuniformities in the fluence or intensity profile of the laser beam. The Contrast Ratio is defined as the  $1\sigma$  standard deviation in the intensity profile divided by its average value. Statistical optics predicts that the contribution to contrast of an optic can be found from  $C = \sqrt{2f}$  where  $f$  is the fraction of light scattered by that optic if  $f$  results from the sum of many small uncorrelated errors, such as would occur from an optic with imperfect optical surfaces.<sup>3</sup>

Contrast calculations performed with our physical optics models that include phase screen descriptions of the individual optics generally agree with this result. The contrast that results from a sequence of optics is the RSS sum of the contrast contributions of each. For fusion-class laser systems a typical contrast specification is 15% or better.

## **2. ARCHITECTURAL EVOLUTION OF ICF LASER BEAMLINE DESIGNS**

Because the impact of large amplitude variations is very high for an ICF laser, for the last 30 years, beamline design has centered around controlling their growth.<sup>4</sup> This control is based on understanding that:

- Diffraction increases amplitude variations as the beam moves away from its near field
- Non-linear driven amplitude variations grow as the beam propagates along its path

As shown in Figure 3, earlier ICF lasers (Shiva, Nova, others) were designed with single-pass Master Oscillator/Power Amplifier (MOPA) chains that held the energy density or fluence constant at the output of each amplifier. This design provided for good energy extraction while staying below the fluence limit for damage. The output from one amplifier was matched to the input of the next amplifier by relay telescopes that served a number of functions. As shown in Figures 3 and 4, they expanded the beam area as required from amplifier to amplifier, they reimaged the near field of the beam at each amplifier, thus reducing the impact of diffraction, and they provided for support of pinholes at the foci of the telescopes. These pinholes are used to strip high-frequency spatial components from the propagating beams.<sup>5</sup>

MOPA chains that were typical of those for Shiva and Nova were characterized by:

- Many different designs for amplifiers and telescopes
- Good gain
- Moderately good extraction efficiency
- Poor packing density
- Low technical risk, no development was needed

When it became clear that inertial confinement fusion ignition was not going to be reached with a laser of the scale of Nova, the search began for a laser design that could provide substantially more output energy at substantially lower cost while continuing to meet all of the requirements for beam quality. LLNL had built a multipass laser in the early 1970's<sup>6</sup>, however this system did not use image relaying and suffered greatly from diffractive and nonlinear propagation effects. A major Russian fusion laser system used a multipass configuration in a total-internal-reflection slab geometry.<sup>7</sup> As early as 1977 the advantages of a multipass image-relayed geometry were beginning to be recognized<sup>8</sup>, however much development was required before it became practical to build a system using this concept. The most appealing approach was to purchase only the largest final amplifiers and use several earlier passes through that amplifier for the required high gain to go from a small master oscillator to the final energy-extracting pass as shown in Figure 1. This multipass chain design is characterized by:

- A single amplifier design
- Good gain
- Good extraction efficiency
- High packing density
- But at the time of its conception, some development was needed

The technologies needing development included an optical switch, a deformable mirror, - frequency conversion crystals, mirrors and polarizers at the largest practical beam area so as to minimize the number of beams in the facility. An amplifier aperture of 40 x 40 cm was chosen as a balance between large size and development risk. All of these components were successfully developed and are now in regular use in NIF.<sup>9</sup> The active element of the switch is a KDP crystal. Voltage must be applied across this switch crystal in the direction of beam propagation, requiring the electrodes to be fully transparent and tolerant of high fluence laser light. Plasma on either side of the crystal provides these electrodes, thus giving rise to the name of the switch, Plasma-Electrode Pockel's Cell (PEPC).<sup>10</sup>

### **3. MULTIPASS PROPAGATION THROUGH A NIF BEAMLIN**

The full implementation for the NIF beamline is shown in Figure 1. In operation the laser pulse is initially generated in a fiber oscillator located in a rack in the master oscillator room (MOR). This single beam is used to generate input for the 192 beams of NIF by an optical system that provides low energy pre-amplification, beam splitting, spectral conditioning and spatial and temporal beam shaping. One of these tailored input beams with polarization in the plane of the paper (P-polarization with respect to the slabs) is injected into a main laser beamline by a small mirror located near the focal plane of the Transport Spatial Filter. The beam is directed through the spatial filter lens, SF3, and into the power amplifier for its first step in high energy amplification. After passing through the power amplifier it is reflected by LM3 and the polarizer through the not-energized PEPC polarization switch. After passing through the Cavity Spatial Filter the beam is amplified once during its first pass through the main amplifier section of the beamline, reflected once by LM1, the deformable mirror and amplified again in the main amplifier as it heads back toward the PEPC. While the laser pulse is inside the main amplifier, voltage is applied to the KDP crystal of the PEPC converting it into a half-wave plate that rotates the polarization of the beam from the plane of the paper to perpendicular to the paper. With its new polarization, the beam is transmitted by the polarizer, (rather than reflected); it is next reflected back towards the polarizer by LM2, transmitted once again through the polarizer and the PEPC where its polarization is rotated back into the plane of the paper. The beam is then amplified by two more passes in the main amplifier and is reflected again by the deformable mirror. This time, while the beam is within the main amplifier, the voltage that was on the PEPC is turned off. When the beam next goes through the PEPC its polarization is unchanged, the beam is then reflected by the polarizer and LM3 and sent on for its last pass through the power amplifier. It makes its last pass through the Transport Spatial Filter and is reflected by the 4 or 5 transport mirrors on its way toward the target chamber. The last transport mirror, LM8, directs the beam radially toward the target at target chamber center.

#### **4. MEETING THE WAVEFRONT REQUIREMENTS FOR NIF**

Meeting the requirements for a NIF beamline is accomplished by a combination of beamline architecture and specifications on individual optics. As previously discussed, beamline design features include incorporation of relay telescopes both to reimaging the near field along the beamline path and to provide a location for pinholes that strip high-frequency spatial noise from the beam. The beamline design also provides a location at LM1 for the deformable mirror that is capable of correcting low-spatial-frequency errors that accumulate along the beamline.

#### 4.1. The Deformable Mirror in the Multipass Architecture

The deformable mirror is a critical element of the multipass architecture.

Without the deformable mirror:

- The impact of pump-induced distortion would be far more difficult to compensate:
  - Different phase front corrections are needed during alignment and during a shot
  - Different phase front corrections are needed for different laser configurations such as 11-7, 11-5, or 11-3
- It would not be possible to adjust the correction for residual thermal distortions in optics that differ for different time periods between shots
- No correction would be possible for thermal non-uniformities in the gas-filled regions along the beamline
- Acquisitions of the large optics with acceptable flatness and homogeneity would be more expensive

Pump-induced distortion is introduced by heating of the laser glass as the flashlamps are fired. As shown in Figure 5 flashlamp heating results in a very slight S-shaped curvature of the slabs that subsequently results in a W-shaped distortion of the phase front of a beam passing through the slabs.<sup>11</sup> Because the NIF beamlines contain many slabs in a multipass configuration, pump-induced peak-to-valley phase plus residual thermal distortion for the entire beamline can be as high as five to seven waves. The NIF deformable mirrors, shown in Figure 6 have an actuator pattern optimized for correcting low-spatial frequency errors expected for NIF optics to the level needed to meet NIF specs for focusable energy and power. Particular emphasis in the choice of actuator configuration was placed on correction of pumped-induced distortion. Note the five actuators across the center of the mirror that match the excursion features of the W-shaped pump-induced wavefront distortion. Each of the individual actuators has a stroke budget of almost 4 waves at 1.053  $\mu\text{m}$ . Because the deformable mirror is used twice in the multipass architecture, and because as a reflector the impact on wavefront for each use is twice the motion of the mirror, the total budget for wavefront correction by the deformable mirror is  $\sim 15$  waves. Because the correction needed from the deformable mirror is only five to seven waves considerable stroke margin is still available.

## 4.2. Specifications for Individual Optics

The specifications that were set for all of the individual optics on NIF were based upon experience gained with earlier fusion lasers at LLNL and the use of design tools developed for these lasers during the years between the early seventies and the early nineties.<sup>12,13</sup> Previous fusion laser systems at LLNL included Janus, Cyclops, Argus, Shiva, Novette and Nova. These testbeds provided many opportunities for interpretation of laser performance from the viewpoints of classical optics, physical optics, and statistical optics using both readily available tools such as Excel, MathCad and IDL and more specialized physical simulations codes developed at LLNL such as PROP and BTGain. These codes were used with candidate wavefront assumptions for the optics to predict wavefront performance of the full NIF system against its Primary Criteria. When necessary, new codes were written to address specific issues of the NIF beamlines, such as the flashlamp induced phase front distortion of the laser slabs, and the performance of the deformable mirror and Hartman sensor package that corrects gradient distortion along the entire beamline. Tradeoffs between cost and performance were completed to assure that performance goals were met for overall minimum cost of the optics.

These studies resulted in a number of categories of wavefront or loss specifications for individual large optics in the NIF beamline. They include specifications for:

- Bulk homogeneity
  - For >2.5 meters of laser glass
  - For >0.5 meters of fused silica
- Bulk absorption
- Losses at transmitting and reflecting surfaces
- Surface figure (for the multipass configuration)
  - For 172 surfaces in transmission
  - For 15 or 16 surfaces in reflection

The bulk homogeneity specs for laser slabs and fused silica optics are being met by the optics accepted for use in NIF. These specs are summarized in Table 1.

A comparison of the passive losses expected for NIF at the time of its design and as the optics are being received is given in Table 2. By far the largest loss is that due to bulk absorption in the KDP material of the PEPC switch. This loss, which is due to intrinsic KDP absorption is  $\sim 6\%$  per pass at  $1.053 \mu\text{m}$ . This loss was accepted at the time of the design of the NIF beamlines.

Years of developmental work and facilitization with coating vendors have resulted in low-loss highly reflective multilayer dielectric coatings for the mirrors and polarizers. Hardened, humidity resistant antireflection solgel coatings for windows, the doubler and the tripler have been developed over the past  $\sim 10$  years at LLNL.<sup>12</sup> These low-loss solgel coatings were chosen rather than multilayer coatings because they also have very high damage resistance. Debris shield losses represent obscurations and transmission losses incurred due to debris from targets.

Surface figure specifications for NIF optics span a large range of spatial wavelengths (or frequencies). Figure 7 compares a number of the features of a NIF beamline on a scale that is consistent with the Power Spectral Density ranges that are used to specify the surface figure for NIF optics. In this figure one can see how the relative dimensions of target features, pinholes, and spot-size goals compare to one another.

The spatial frequency ranges used for specification of the NIF 1 $\omega$  optics are given in Figure 8. These ranges are defined by the spatial frequencies that are accessible by particular diagnostic instruments. The fractional area of the optic that is sampled by a diagnostic is a function of the size of the feature being studied. The entire optic is tested using a transmitted wavefront measurement when evaluating whether or not an optic meets its RMS Gradient or PSD-1 spec. Much smaller regions of the surfaces are sampled for evaluation of the PSD-2 or Roughness specs. For these two, a set of 9 samples in a 3 x 3 tic-tac-toe pattern are typically measured for each surface.

The wavefront specifications for large “glass” NIF optics are shown in Figure 9. These large glass optics include laser slabs, transport mirrors and fused silica optics. The rms Gradient spec is represented by the value;  $< 7\text{nm/cm}$ . Both a Not-to-Exceed line and rms values are specified for the PSD and Roughness regions. Figure 9 also presents the maximum fraction of the light that is scattered within each region, for an optic that meets spec.

The Gradient region highlighted in Figure 10 controls the minimum spot size that can be achieved at target chamber center. Much of the error within this band is correctable with the deformable mirror.

The actual spot size desired for NIF differs with differing missions. Spot size goals for these missions were formally reviewed most recently in Reference 15. The original spot size requirement for the Indirect Drive ICF mission, included in the NIF Primary Criteria and Functional Requirements Document is that the laser output should be delivered into a 600  $\mu\text{m}$  diameter circle. As the thinking of ICF target designers has matured, their goal for spot size has changed somewhat, to a 500  $\mu\text{m}$  x 1000  $\mu\text{m}$  ellipse, smoothed with the aid of a  $1\omega$  CPP and frequency modulation on the beam. We expect these spot size goals to continue to evolve. The spot size goals of the Stockpile Stewardship Program (SSP) have been described in terms of a circle with a diameter that is a function of the fractional energy delivered to that circle, as shown in Figure 11.<sup>15</sup>

The character of a NIF spot at the target location can be modified considerably with the use of phase plates and beam modulation to meet the needs of specific targets. Figure 12 illustrates the speckle pattern at the best focus (with an active deformable mirror) calculated by PROP for the  $3\omega$  beam for a set of NIF baseline optics with no phase plate present. This energy can be spread into the elliptical spot goals with beam smoothing (Figure 13) for ICF by inserting an appropriate phase plate into the  $1\omega$  beam and increasing the modulation at  $1\omega$  to 17 Ghz, resulting in a total modulation driven wavelength spread of the  $1\omega$  laser of  $\sim 3 \text{ \AA}$ .

Meeting the SSP spot size goal requires use of the deformable mirror. The current 39 actuator design was chosen on the basis of spot size calculations for designs with 23, 39, 59, 68, 105, 449 and 1033 actuators. The 39 actuator design was effective at meeting requirements; only  $\sim 15\%$  spot size improvements were calculated for the more complex and expensive 59 and 68 actuator options.

Our attention is next directed toward the PSD-1, PSD-2 and roughness bands. Energy in these bands represents high spatial frequency noise that feeds amplitude variations on the beam. Figure 14 illustrates the importance of the pinholes at the foci of the spatial filters. Energy in the low spatial frequency end of the PSD-1 region can get through the

pinholes, while energy in the high spatial frequency region of the PSD-1 band and all of the energy in the PSD-2 and roughness bands is stripped by the pinholes. Optics that have good beamline performance in the PSD-1 band result in low energy scattered in this band. With good PSD-1 optics, the NIF operator has more freedom to use a larger pinhole. With larger pinholes, alignment tolerances and the threat of pinhole closer due to a small misalignment error in the pinhole are both less severe. Thus better  $1\omega$  optics result in a  $1\omega$  laser that is significantly easier to align and operate.

Wavefront specifications for crystals and measured values for early crystals delivered to NIF are shown in Figure 15.<sup>17,18</sup> The ability of crystals to meet this RMS Gradient spec is driven by both material homogeneity and the capability of the diamond turning machine. Typically the contribution to RMS Gradient from each is nominally 50/50. PSD-1, PSD-2 and Roughness specifications for crystal optics are consistent with the capabilities of the diamond turning machines. Crystals now being produced are meeting and exceeding these specs.

The impact on contrast along the beamlines is calculated by the NIF propagation code, PROP. Typically 512 x 512 pixel PROP calculations of the full beam cross-section include the effects of the gradient and PSD-1 bands. With today's computers, these runs take 20 to 30 minutes each. When the specs for NIF optics were being developed they would take 4 to 8 hours.

To evaluate the impacts of scattering in the PSD-2 and roughness bands PROP is used in what is referred to as a patch calculation. The PROP grid size ranges from ~512 x 512 to 2048 x 2048; in this case, however a much smaller area of the beam is studied, corresponding to the size of the PSD-2 and roughness features.

Full area beamline calculations using PROP can predict the expected focal spot size. However, contrast or amplitude modulation results are found from the RSS sum of full-beam and patch calculations.

Comparison of the impact of the wavefront specifications placed on NIF  $1\omega$  optics and those that are measured for received optics can be quickly comprehended with plots of the last-pass cumulative value of the 1D PSD for each of the specified regions, Gradient to Roughness, shown by encounter with each individual optic as the laser would move along

the beamline. Figure 16 shows comparisons of these cumulative values as calculated from NIF specs and as calculated from typical offline measurements of received optics.

## **5. DEFINITION OF THE CLEANLINESS SPECIFICATIONS FOR THE $1\omega$ PORTION OF THE NIF BEAMLINE**

The impact of obscurations on optics in the  $1\omega$  portion of the NIF laser depends on the dimensions of the obscuration. Small obscurations scatter light over a large range of spatial frequencies leading to increased contrast in the downstream beam. Larger obscurations put well-defined structure on the amplitude profile of the beam that can subsequently lead to downstream hot-focusing.<sup>19</sup> The line between small and large obscurations is determined by the size of the pinholes that are in the beamline. For 100  $\mu$ rad pinholes, small particles are  $\leq 1.5$  to 2 mm in diameter. For 200  $\mu$ rad pinholes, they are less than 0.5 to 1 mm. A useful rule of thumb for determining whether or not a given obscuration will be problematic from the hot-focusing point of view is: diameter of obscuration in mm times half-angle of spatial filter  $\leq 200$  mm- $\mu$ rad. If a downstream hot-focused spot should fall on an optical surface, it can initiate and drive the growth of damage on that surface.

Obscurations in the  $1\omega$  portion of the laser typically originate because dirt particles are deposited on the laser slabs.<sup>20</sup> Upon firing of the flashlamps, the dirt particles become hot enough to form a plasma, permanently scarring the surface of the slab. These scars typically do not grow upon subsequent illumination by the laser beam. From the work of J. Menapace, the size of the obscuration after flashlamp irradiation is assumed to be  $\sim 7$  times the size of the original dirt particle.<sup>21</sup> Flowdown from the basic requirements for NIF to requirements for cleanliness along the beamline was completed using the following assumptions:

- The distribution of sizes of obscurations on laser slabs expected for NIF was assumed to be the same as that shown in Figure 17 for Beamlet slabs at the end of its use (EOU) at LLNL. The Beamlet distribution is very similar to that found for Nova.<sup>21</sup>
- The total number of obscurations could differ for NIF compared to that found for Beamlet

- The obscurations were assumed to “absorb” all incident laser light, thus they affected only the amplitude of the incident beam, not its phase

These assumptions were converted into an equivalent PSD for the small obscurations in the following manner:

- Select an appropriately small bin size for describing the size distribution of the obscurations
- Take the Fourier transform of the obscuration of each bin (This is roughly equivalent to observing the intensity pattern of a focused near-uniform intensity profile that had zero amplitude over the area of the obscuration)
- Incoherently add the Fourier transform of all of the obscuration bins, weighted according to the distribution of sizes found for Beamlet. (This incoherent addition is appropriate because there are a large number of small obscurations with no particular phase relationship with each other.)

This incoherent sum represents the effective PSD of the obscuration distribution and allows cleanliness requirements to be compared directly to optical specifications. It also goes a long way toward overcoming the practical limitations on computer memory and computational time that appear as soon as actual obscuration scale sizes are included in full aperture laser system simulations.

Figure 18 compares Beamlet end-of-use obscurations expressed on a per slab basis with the optical specifications for NIF glass optics. If NIF laser slabs were to experience dirt contamination at the level of that observed on Beamlet, the impact on  $1\omega$  contrast along the beam for a baseline ICF target shot would be negligible compared to the impact of imperfections on the optics. In fact, however efforts during construction and preliminary operations to keep beamlines clean have been very successful. NIF slabs have many fewer obscurations than experienced for Beamlet, and we have observed no significant decrease in cleanliness level as we continue with commissioning shots. To a large extent, this success at maintaining a high level of cleanliness together with high optical quality in the PSD-2 and Roughness regimes has led to the excellent high-power performance demonstrated during NIF commissioning.

## **6. INTEGRATED BEAMLINER PERFORMANCE**

The many optical and cleanliness requirements described above were all centered around delivering focusable energy and power.<sup>22,23</sup> A 1 $\omega$  far-field focal spot profile measured for a full power, full system shot is given in Figure 19, next to our estimate of the total PSD for beamline 315. This estimate includes the impact of not only all of the optics in beamline 315; it also includes the impact of thermal non-uniformities in the atmosphere (air and argon) of the beamline and the impact of any non-linear effects that are present for a full-power system shot. The abrupt truncation of this PSD at  $\sim 5\text{mm}^{-1}$  is due to limitations in the resolution of the measurement and is not physical.

Early NIF beamlines have delivered 80% of their output power within 16  $\mu$ rad, surpassing their goal of 80% within 18  $\mu$ rad. During this past year, NIF has fired over 500 beamline shots, demonstrating again and again that the architectural strategy and selection of specs for individual optical components were appropriate for meeting its primary criteria.

## **7. SUMMARY**

The flowdown from the NIF Primary Criteria and Functional Requirements to specifications for optics has been well understood for the NIF Project. In general, the large optics being delivered are meeting or beating their specs. Margin in one area has often been used to accommodate for minor problems in other areas. The system has now been tested as fully integrated beamlines. Performance during the integrated tests has verified that the strategy chosen for the NIF optical system provided an appropriate balance between minimum cost and achieving performance that meets (and somewhat exceeds) the goals for the Project.

## **ACKNOWLEDGEMENTS**

The authors listed for this paper are those that directly contributed to the documentation provided for this article. In fact, however the concepts described herein represent the integrated evolution of thought of a much larger set of NIF authors too numerous to list. The set of people who probably deserve the most credit for developing these concepts are those that contributed to the NIF CDR, written between 1992 and 1994.<sup>24</sup> This work performed under the auspices of the

U.S. Department of Energy, National Nuclear Security Administration by the University of California Lawrence Livermore National Laboratory under Contract No. W-7405-Eng-48.

## REFERENCES

1. Inertial Confinement Fusion, J. Lindl, AIP Press, Springer (1998)
2. W. H. Williams et al., "Optical Propagation Modeling", these proceedings
3. K.R. Manes, W. W. Simmons "Statistical optics applied to high-power glass lasers" *JOSA A* **2** 528-538 (1985)
4. W. W. Simmons, J. T. Hunt, and W. E. Warren, "Light propagation through large laser systems, " *IEEE J. Quantum Electron.* **QE-17**, 1727-1744 (1981)
5. J. T. Hunt, J. A. Glaze, W.W. Simmons, and P. Renard, "Suppression of self-focusing through low-pass spatial filtering and relay imaging, *Applied Optics* **17**. 2053-2057 (1978)
6. S. W. Mead, R. E. Kidder, J. E. Swain, F. Rainer, and J. Petruzzi, "Preliminary measurements of x-ray and neutron emission from laser-produced plasmas," *Applied Optics* **11**, 345-352 (1972)
7. M. E. Brodov, V. P. Degtyarova, A. V. Ivanov, P. I Ivashkin, V. V. Korobkin, P. P. Pashinin, A. M. Prokhorov, and R. V. Serov, "A study into characteristics of a triple-pass amplifier using a neodymium glass slab, " *Kvant. Elekt.* **9**, 121-125 (1982)
8. LLNL Laser Program Annual Report 1977, pages 2-3 to 2-5, UCRL-50021-77
9. B. M. Van Wonterghem, J. R. Murray, J. H Campbell, D. R. Speck, C. E. Barker, I. C. Smith D. F. Browning and W. C. Behrendt "Performance of a prototype for a large-aperture multipass Nd:glass laser for inertial confinement fusion, " *Applied Optics* **36**, 4932-4953 (1997)
10. M.A. Rhodes, B. Woods, J. J. DeYoreo, D. Roberts, and L. J. Atherton "Performance of large-aperture optical switches for high-energy inertial-confinement fusion lasers," *Applied Optics* **34**, 5312-5325 (1995).
11. A. C. Erlandson, (ed.) " Physics basis for optical performance of the NIF amplifiers," NIF document NIF-0014142 0A (Jan 11, 1999)

12. J. K. Lawson, D. M. Aikens, R. E. English, Jr., and C. R. Wolfe, "Power spectral density specifications for high-power laser system," in *Specifications, Production, and Testing of Optical Components and Systems*, A. E. Gee and J. Houee, eds., *Proceedings of SPIE* Volume **2775**, 345-356 (1996)
13. J. Walsh, A. J. Leistner, and B. F. Oreb "Power spectral density analysis of optical substrates for gravitational-wave interferometry", *Applied Optics* **38 No. 22** 4790-4801 (1999)
14. I. M. Thomas, A. K. Burnham, J. R. Ertel, and S. C. Frieders, iMethod for reducing the effect of environmental contamination of sol-gel optical coatings, *Proceedings of SPIE* Volume **3492**; *Third Annual International Conference on Solid State Lasers for Application to Inertial Confinement Fusion*, 220-229 (1998); E. K. Wheeler, J. T. McWhorter, P. K. Whitman, C. Thorsness, J. DeYoreo, I. M. Thomas, and M. Hester, *Proceedings of SPIE* Volume **3902**, 451 (1999).
15. W. H. Williams, J. M. Auerbach, M. A. Henesian, J. K. Lawson, P. A. Renard, R. A Sacks "The NIF's basic focal spot for temporally flat pulses", & "The NIF's basic focal spot for ICF temporally shaped pulses", *NIF Laser System Performance Ratings; Supplement to Proceedings of SPIE* Volume **3492**; *Third Annual International Conference on Solid State Lasers for Application to Inertial Confinement Fusion*. 22-38 & 55-60 (1998)
16. W. H. Williams, private communication
17. P. J. Wegner, J. M. Auerbach, C. E. Barker, S. C. Burkart, S. A. Couture, J. J. DeYoreo, R. L. Hibbbad, L. W. Liou, M. A. Norton, P. A. Whitman and L. A Hackel, "Frequency converter development for the National Ignition Facility" *Proceedings of SPIE* Volume **3492**, 392-405 (1998)
18. P. K. Whitman and W. H. Williams, private communication
19. J. T. Hunt, K. R. Manes, and P. A. Renard, "Hot images from obscurations," *Applied Optics* **32** 5973-5982 (1993)
20. I. F. Stowers, H. G. Patton, "Damage History of Argus, a 4 TW Nd-Glass System", *Symposium on Optical Materials for High Power Lasers*, Boulder, CO, 4 Oct 1977 (UCRL-80419)
21. I.F. Stowers, J. A. Horvath, J. A Menapace, A. K. Burnham, S. A. Letts, "Achieving and Maintaining Cleanliness in FIF Amplifiers", *SPIE, Third Annual International Conference on Solid State Lasers for Applications to Inertial Confinement Fusion*, Monterey, CA June 7-12, 1998, UCRL-JC-130040
22. C. C. Widmayer, N. C. Mehta, and W. H. Williams, "NIF 11-5 Baseline Model Performance Summary," NIF document NIF-0078913-OA, March 5, 2002

23. B. M. Van Wonterghem, S. C. Burkhart, C. A. Haynam, K. R. Manes, C. D. Marshall, J. E. Murray, M. L. Spaeth, D. R. Speck, S. B. Sutton, P. J. Wegner, "NIF Commissioning and Initial Performance Results," UCRL-CONF-155818, SPIE, Photonics West - LASE 2004 Conference, San Jose, CA, January 24-29, 2004.

24. Laser Design Basis, DE 94016700 UCRL-JC-117399 (1994)

Figure Captions:

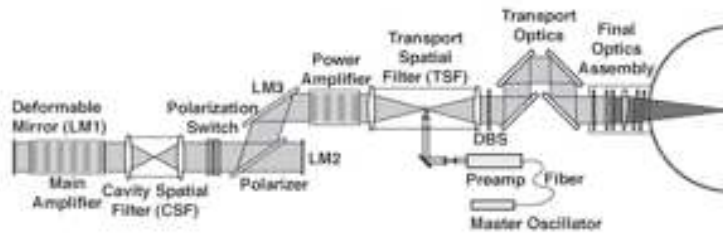


Figure 1. The multipass architecture that is common to all of the 192 beamlines of NIF. There are four passes through the main amplifier and two passes through the power amplifier. Laser glass slabs are mounted in the amplifiers oriented vertically and set at Brewster's angle. Not shown in this figure is the Hartmann Sensor closed-loop feedback circuit that, as part of the output sensor package located in the transport spatial filter, controls the deformable mirror for wavefront correction.

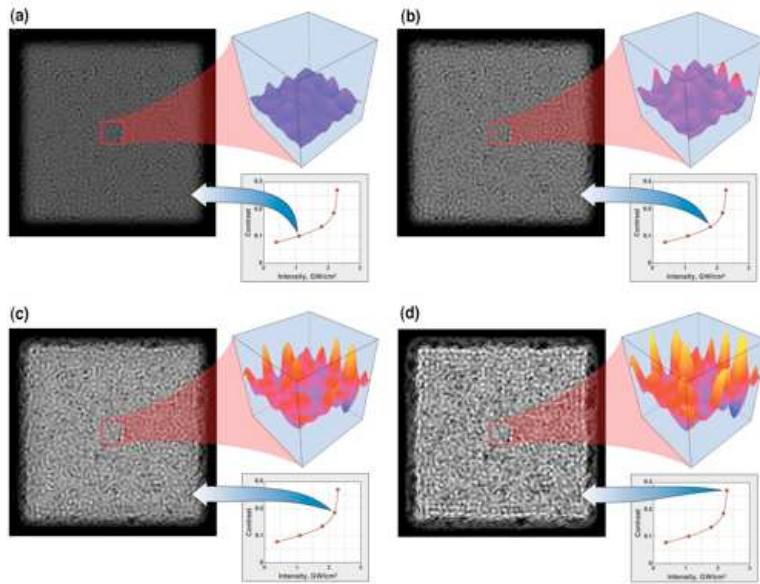


Figure 2. This sequence of four images illustrates the growth of amplitude non-uniformities in the spatial profile of a large ICF laser as the intensity of the beam is increased.

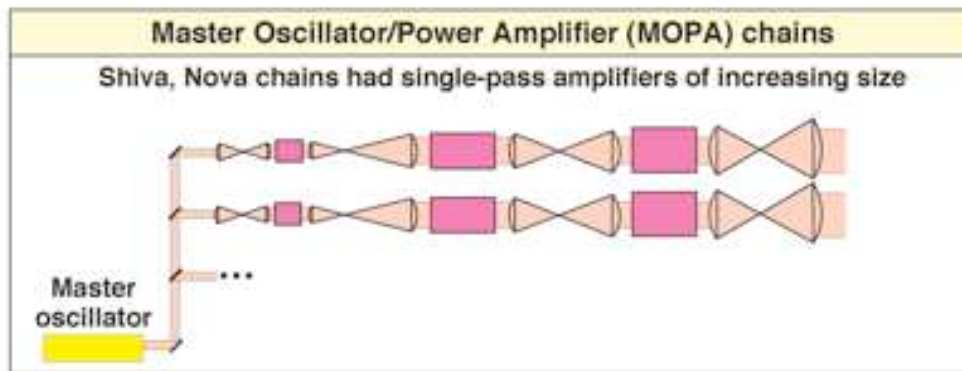


Figure 3. A typical ICF single pass laser chain architecture for lasers designed in the time frame between the early seventies and the early nineties. Note that the clear aperture of the amplifiers increases as the beam moves down the chain.

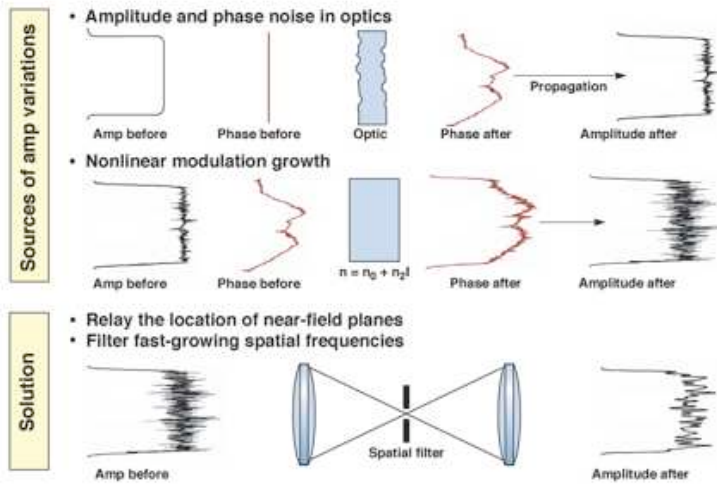


Figure 4. Spatial filters at intervals within a solid-state amplifier chain interrupt the parasitic growth of non-focusable high spatial frequency modes.<sup>5</sup>

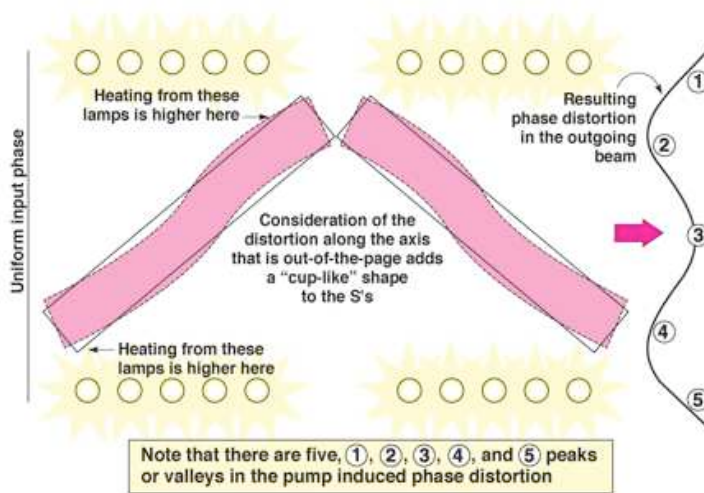


Figure 5. Looking down from the top; an exaggerated view of the distortion that is introduced into the laser slabs when they are illuminated by the pulse of light from the flashlamps.

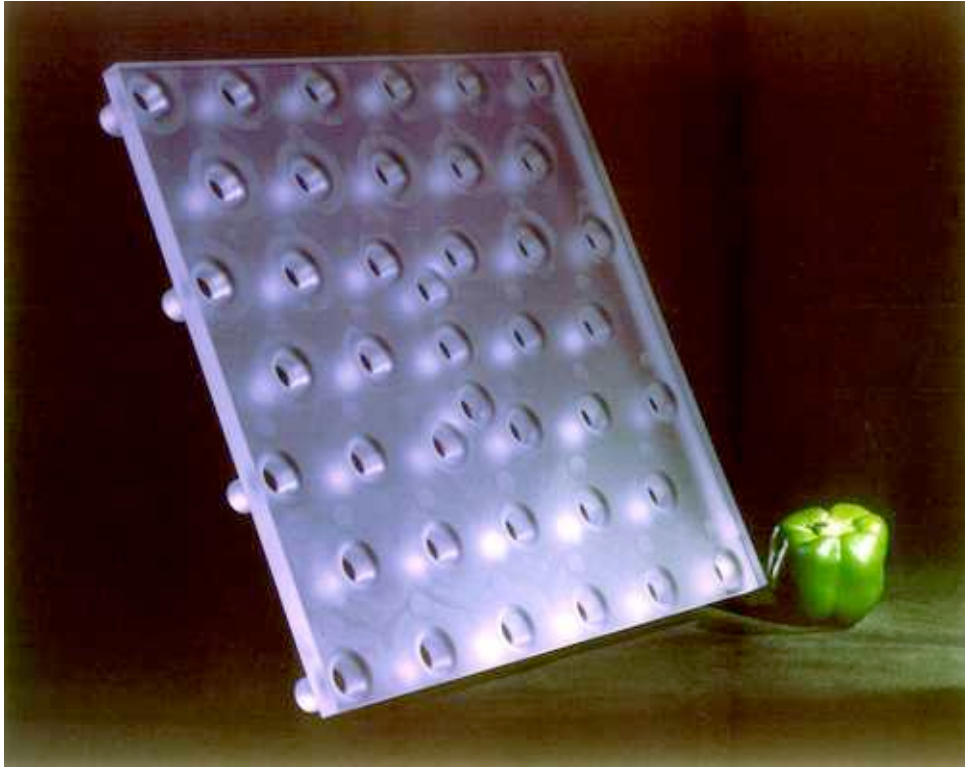


Figure 6. The deformable mirror optic of NIF with its 39 actuator attachment points. When mounted in NIF, the mirror is positioned vertically at the end of the main amplifier cavity with the actuator orientation as shown.

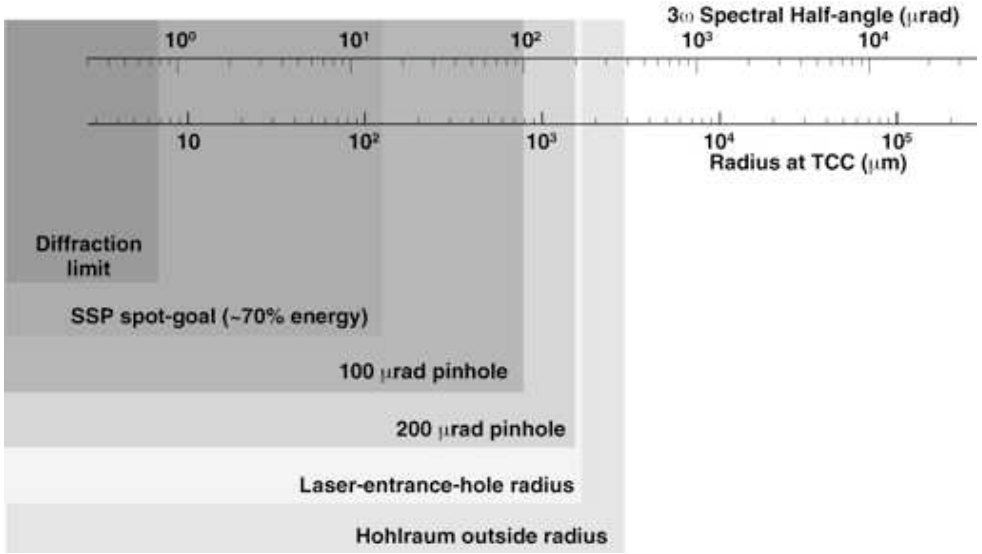


Figure 7. Comparison of a number of the features of a NIF beamline on a scale that is consistent with Power Spectral Density ranges that will be subsequently used to characterize the specifications for NIF optics.

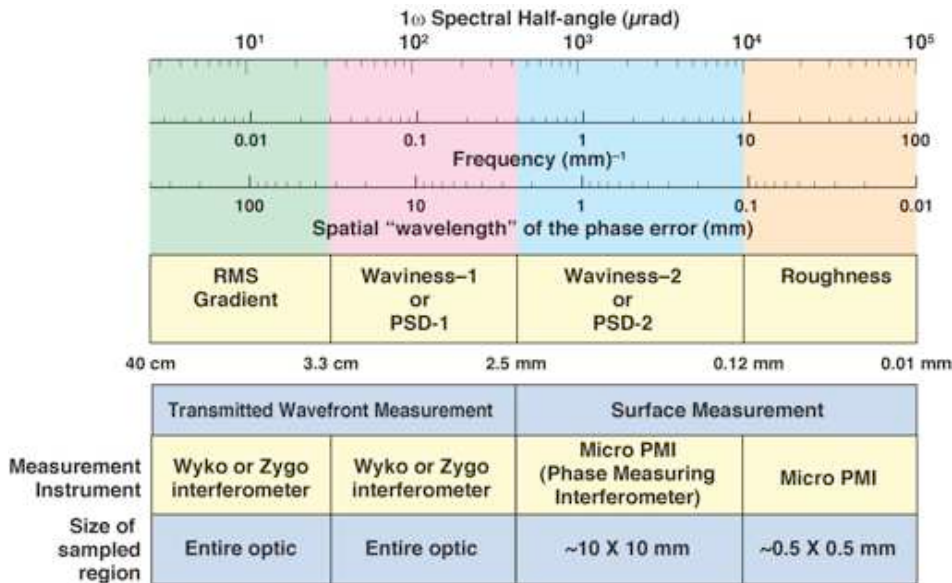


Figure 8. The spatial frequency or spatial wavelength ranges that are used to specify the optical quality required of NIF optics. The different ranges are delineated from each other in terms of the diagnostics instruments used to measure features in each range.

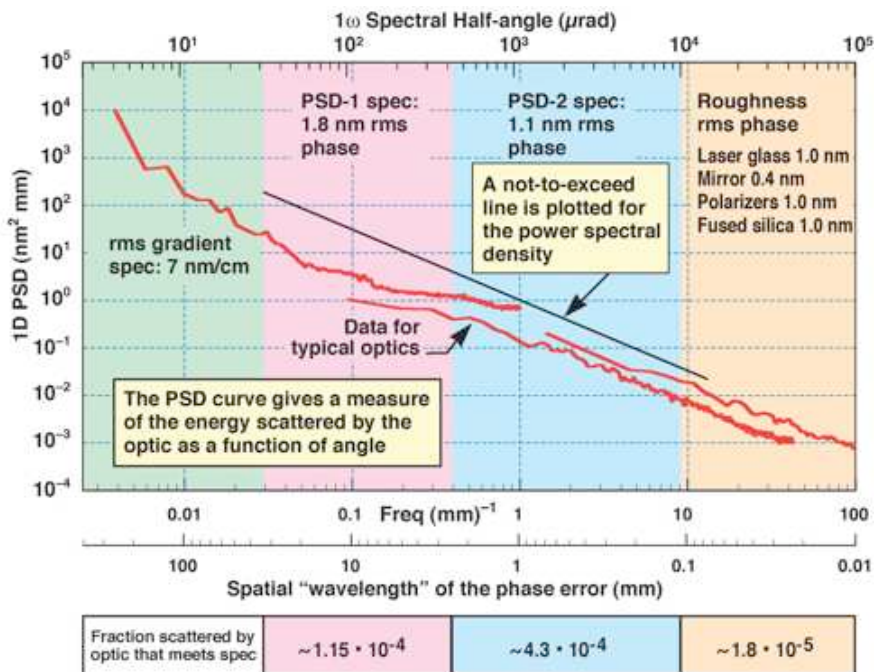


Figure 9. Specifications used for the large glass optics of NIF expressed in terms of their 1D PSD. There are two types of specification for the PSD-1, PSD-2 and Roughness ranges, a specification for the rms value over that range, and a not-to-exceed value that is a function of spatial frequency.

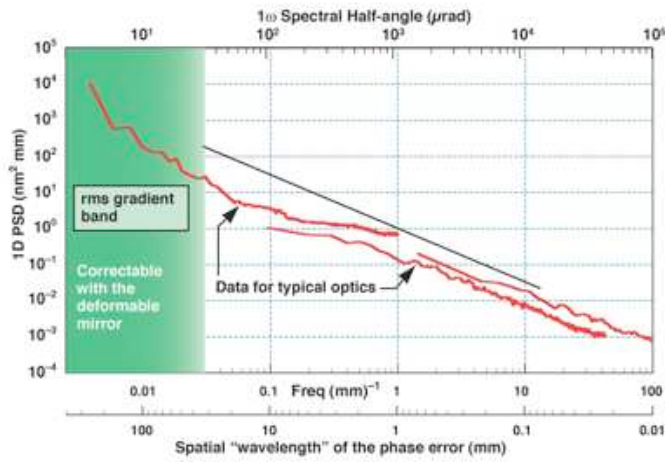


Figure 10. The gradient region does not have a not-to-exceed specification. It has an rms spec of 7nm/cm. The spatial frequencies within this range are those that determine the spot size of the focused beam on target.

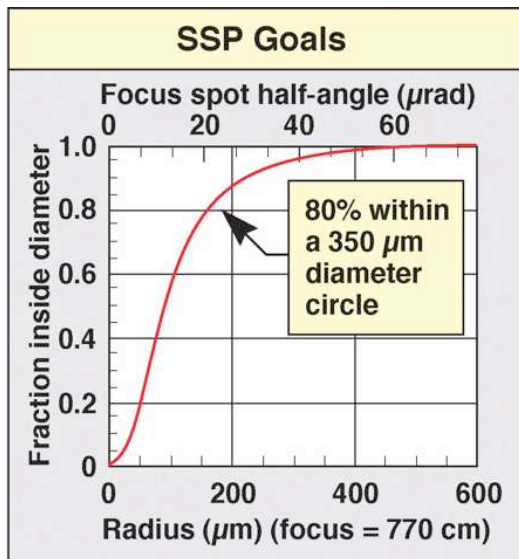


Figure 11. The Stockpile Stewardship spot size goals for NIF have been expressed in terms of the fractional output energy or intensity delivered within that diameter.

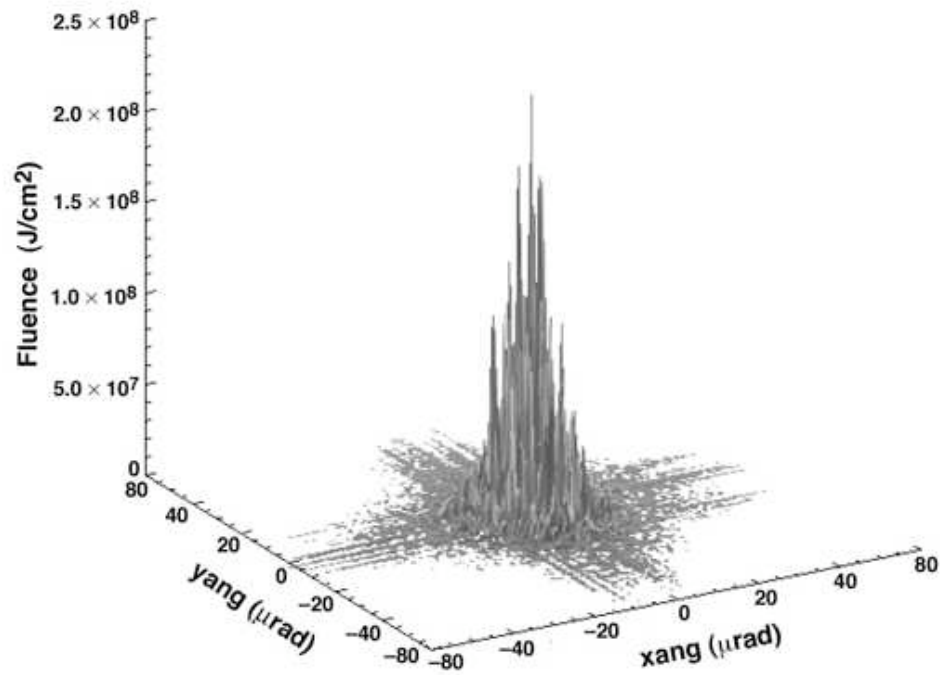


Figure 12. The calculated character of the focused spot produced by a baseline NIF beam at baseline energy with no  $1\omega$  CPP in the beam.<sup>16</sup>

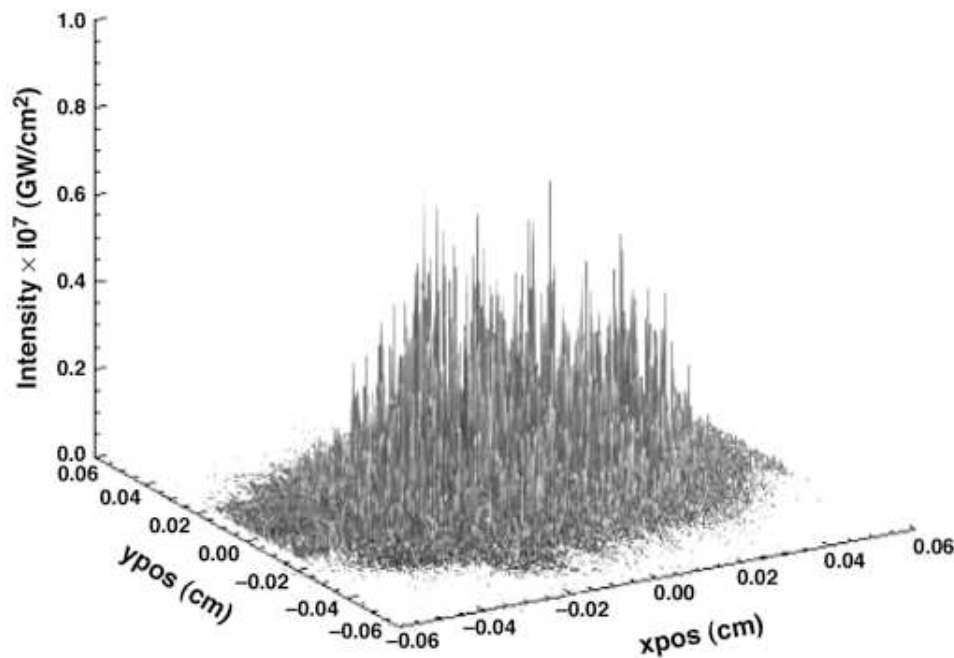


Figure 13. The calculated character of the focused spot produced by a baseline NIF beam at baseline energy with an appropriate  $1\omega$  CPP designed to produce a 500 μm by 1000 μm elliptical spot.<sup>16</sup>

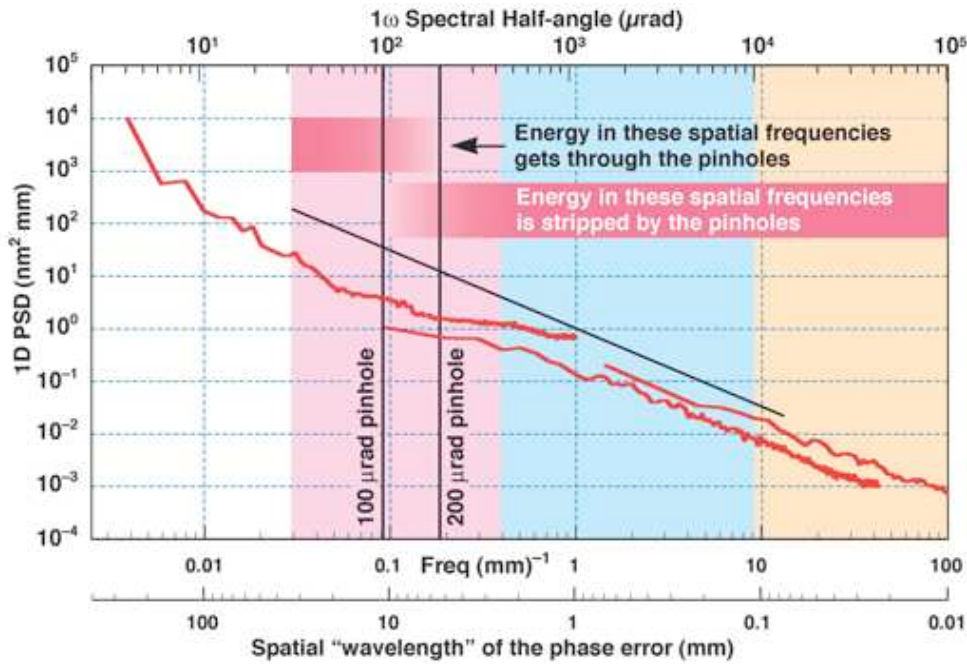


Figure 14. The relationship between the PSD-1, PSD-2 and Roughness bands and the cut off spatial frequencies of possible NIF spatial filter pinholes.

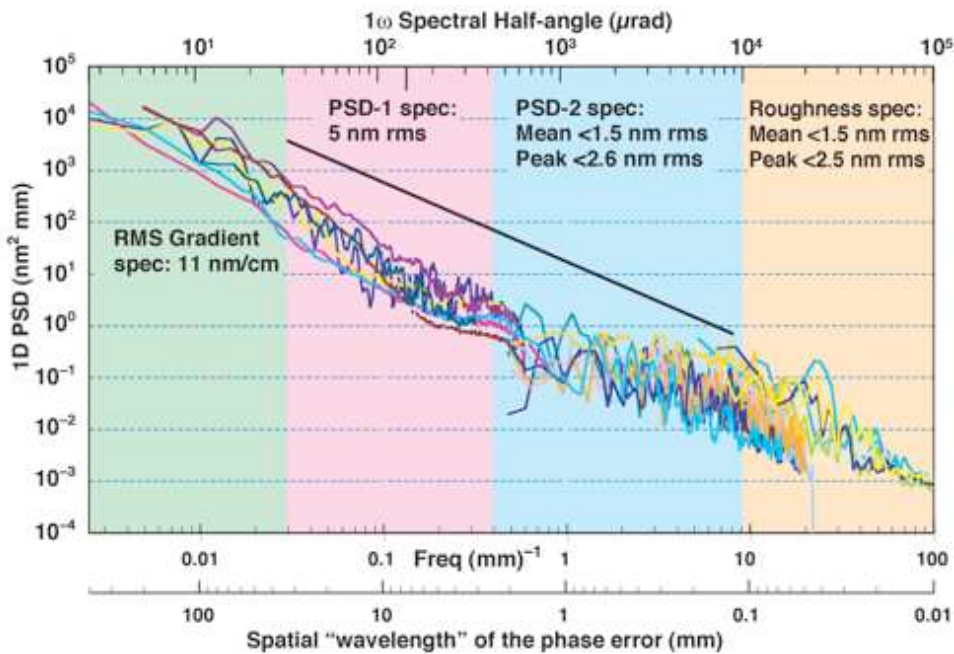


Figure 15. Specifications used for the large crystal optics of NIF expressed in terms of their 1D PSD. These specifications result from consideration of the ability of vendors to grow and diamond finish crystals and the integrated need for a focusable beam after its multipass trip through the beamline.<sup>18</sup>

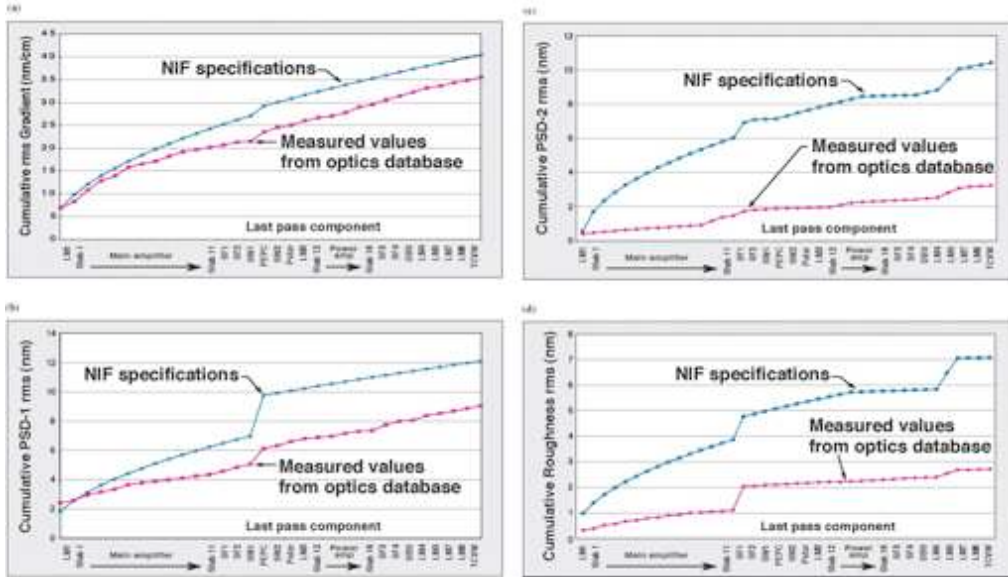


Figure 16. The cumulative value of the rms PSD in each of the four ranges, calculated by encounter with each individual optic along the path the laser pulse takes as it moves through its *last pass* down the beamline, where each optic is different.

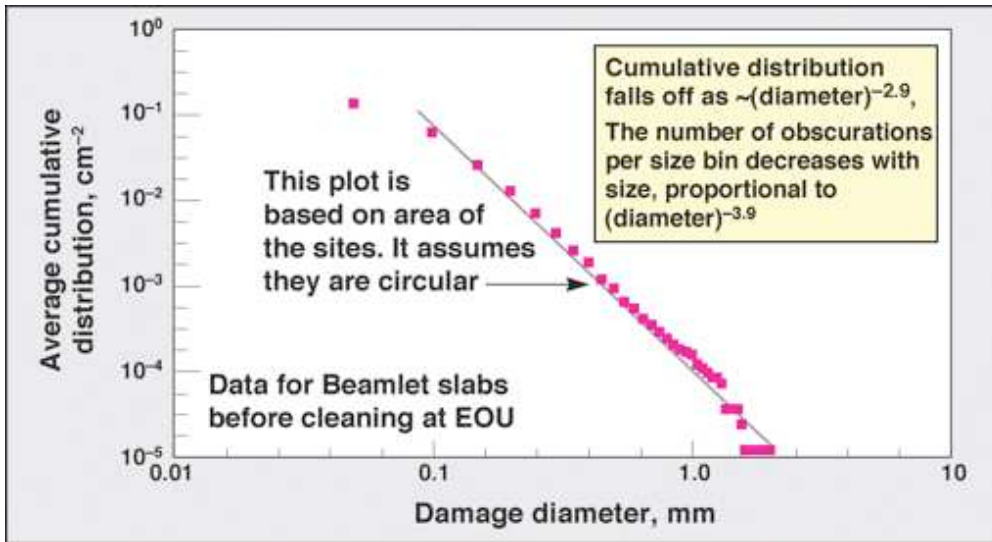


Figure 17. The average cumulative distribution of sizes for dirt/damage sites measured for Beamlet slabs at the end of its use at LLNL.

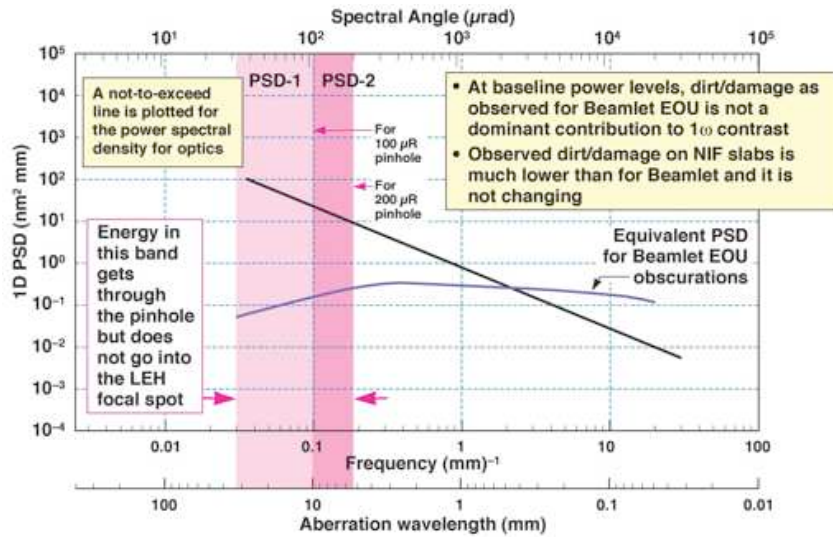


Figure 18. Calculated equivalent PSD for a dirt/damage distribution of sizes given by that for Beamlet in Figure 18. More or less dirt/damage sites will proportionally move the equivalent PSD up or down, as long as the relative distribution stays the same.

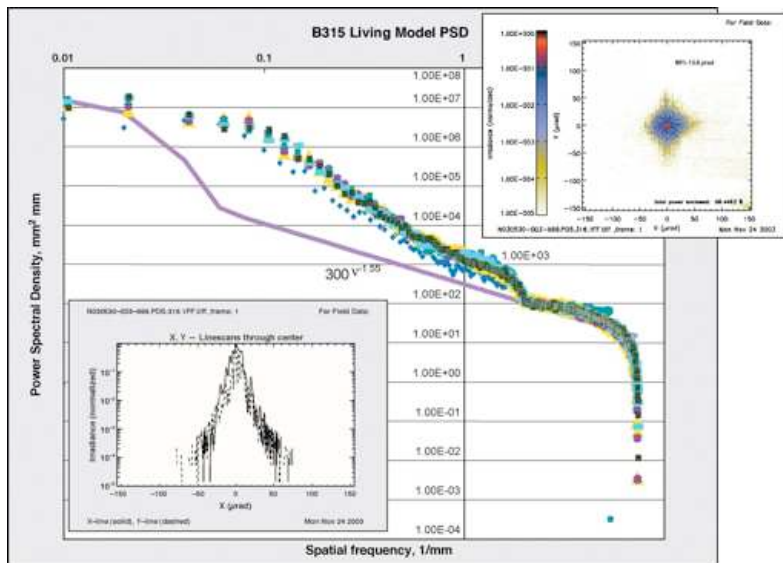


Figure 19. A three part summary of NIF wavefront performance. Part 1; The total PSD for the entire beamline calculated by PROP with inputs of the metrology files for all of the optics, all saturated gain profiles, all thermal induced distortion including gas motion, the residual error from the deformable mirror and all linear and non-linear diffraction effects. Part 2; the measured  $1\omega$  far-field fluence of the beam. And Part 3; x and y lineouts of the measured far-field fluence profile.



Table Captions:

Table 1: Bulk homogeneity specifications for NIF optics

Table 2: Passive losses for NIF large optics